Biochemical and Biophysical Research Communications 543 (2021) 65–71

Contents lists available at ScienceDirect

Biochemical and Biophysical Research Communications

journal homepage: www.elsevier.com/locate/ybbrc

Strain-specific clearance of seed-dependent tau aggregation by lithium-induced autophagy

Mohammad Nasir Uddin [a], Montasir Elahi [a, b], Shotaro Shimonaka [a, c], Soichiro Kakuta [d], Koichi Ishiguro [b], Yumiko Motoi [a, b, c, *], Nobutaka Hattori [a, b, c]

[a] Department of Diagnosis, Prevention and Treatment of Dementia, Graduate School of Medicine, Juntendo University, Tokyo, Japan
[b] Department of Neurology, Graduate School of Medicine, Juntendo University, Tokyo, Japan
[c] Research Institute for Diseases of Old Age, Graduate School of Medicine, Juntendo University, Tokyo, Japan
[d] Laboratory of Morphology and Image Analysis, Research Support Center, Graduate School of Medicine, Juntendo University, Tokyo, Japan

ARTICLE INFO

Article history:
Received 19 December 2020
Accepted 22 December 2020
Available online 28 January 2021

Keywords:
Tau
Aggregation
Autophagy
Lithium
IMPase
Conformation

ABSTRACT

Different conformational strains of tau have been implicated in the clinicopathological heterogeneity of tauopathies. In this study, we hypothesized that distinct strains are degraded in a different manner. Lithium, a drug for bipolar disorder, had previously been reported to reduce aggregation-prone protein content by promoting autophagy. Here, we assessed the effects of lithium on tau aggregates using different tauopathy brain seeds. SH-SY5Y cells were transfected with C-terminal tau fragment Tau-CTF24 (residues 243–441), and Alzheimer's disease (AD), progressive supranuclear palsy (PSP), and corticobasal degeneration (CBD) brain seeds were introduced. After 48-h lithium treatment, sarkosyl-insoluble fractions were prepared. Lithium treatment was found to reduce the amount of insoluble tau and p62, and increase LC3-II levels along with the number of autophagic vacuoles in AD-seeded cells. The effects were lower in case of CBD seeds, and comparable between PSP and AD seeds. An inhibitor of *myo*-inositol monophosphatase (IMPase) also demonstrated similar effects. Overall, the study suggested that aggregated tau protein is degraded by lithium-induced autophagy, influencing IMPase in a strain-specific manner.

1. Introduction

Accumulation of aggregated tau protein is the major neuropathological hallmark of several neurodegenerative tauopathies, including Alzheimer's disease (AD), corticobasal degeneration (CBD), and progressive supranuclear palsy (PSP) [1]. In AD, pathological tau aggregates comprise of paired helical filaments or straight filaments assembled from all six tau isoforms in neurons [2]. In CBD and PSP, mainly 3 isoforms with 4 microtubule-binding repeats in the carboxy-terminal (4R) of tau accumulate in neurons and glial cells; however, the pattern of low-molecular-weight bands of insoluble tau varies between the two [3]. Morphology of the filaments also differs, most being twisted in PSP and straight in CBD [4].

Several recent studies, including ours, have reported pre-existing tau aggregates to act as "seeds" for the aggregation of soluble tau; the resulting pathological aggregates propagate across cells through transmission of these proteopathic tau seeds [5,6]. Injection of tau extracts from postmortem brains of patients with AD, PSP, and CBD into the brain of non-transgenic mice induced differences in cell-type specificity of tau aggregate transmission, demonstrating PSP and CBD tau to induce glial transmission, which is reminiscent of the human pathology [7–9]. These findings led to the strain hypothesis, which suggested that prion-like propagation of unique structural conformations (strains) accounts for the neuropathological heterogeneity of tauopathies [10,11]. Recent cryo-EM analyses have revealed that high-resolution structures of AD tau filaments are different from those of CBD [12–14], thereby collectively suggesting that distinct tau strains could influence the tau degradation system differently.

Two important intracellular degradation machineries have been

Abbreviations: AD, Alzheimer's disease; AVs, Autophagic vacuoles; CBD, Corticobasal degeneration; PSP, Progressive supranuclear palsy; IMPase, *myo*-Inositol monophosphatase.

* Corresponding author. Department of Diagnosis, Prevention, and Treatment of Dementia, Juntendo University Graduate School of Medicine, 3-1-3, Hongo, Bunkyo-ku, Tokyo, 113-8421, Japan.
E-mail address: motoi@juntendo.ac.jp (Y. Motoi).

https://doi.org/10.1016/j.bbrc.2020.12.113
0006-291X/

reported to be associated with the elimination of tau protein aggregates and deformed proteins; they include the ubiquitin-proteasome system and the autophagy lysosome pathway [15,16]. Tau aggregates and phosphorylated forms of tau are degraded by autophagy [17]. Alteration of autophagy in neurodegenerative diseases had previously been suggested as a potential therapeutic strategy [16,18]. Lithium, which is used to treat bipolar disorders, has also been reported to alter autophagy under various conditions [19]. Using cell culture models of neurodegenerative diseases, lithium has been found to increase the degradation of aggregate-prone proteins, such as mutated huntingtin, α-synuclein, and prion protein [20,21]. We hypothesized that distinct strains of tau protein might be degraded differently in lithium-induced autophagy. In this study, we investigated lithium-induced tau aggregate clearance in human brain seed-dependent cell models using various brain samples of patients with AD, PSP, and CBD.

2. Materials and methods

2.1. Preparation of human tauopathy brain seeds

Human brain samples were obtained from the brain bank of Juntendo University Hospital. All experimental procedures using human brain samples were approved by the ethics committee of Juntendo University School of Medicine (approval number: 2012068). Samples from patients with pathologically confirmed tauopathies, including the frontal cortices in case of AD (n = 3), pons in case of PSP (n = 3), and frontal cortices in case of CBD (n = 3), were used for seed preparation; all related information is described in Table S1. Frozen brain tissues were cut into 0.2-g blocks and immediately homogenized in 2 mL of A68 buffer (10 mM Tris-HCl pH 7.5, 10% sucrose, 0.8 M NaCl, and 1 mM EGTA) using a Dounce homogenizer. Lysates were sonicated using an ultrasonic homogenizer (VP−050 N, TAITEC Corporation, Japan) for 1 min (power 25.0%) and centrifuged at 3,000×*g* for 10 min at 4 °C. The supernatants were collected and stored at −80 °C and pellets were discarded [22].

2.2. Cell culture, transfection, and seed induction

SH-SY5Y cells were cultured in Dulbecco's modified Eagle's medium/F12 DMEM (Merck, Germany) supplemented with 10% fetal calf serum at 37 °C. Cells were grown to 80% confluence in collagen-coated 6-well culture dishes (Merck), and used for transfection and seeding thereafter [22]. Transfection of expression plasmid (pcDNA3_Tau-CTF24 [Fig. S1A] or pcDNA3_4R2N-tau [Fig. S3A] [6]) was performed using X-tremeGENE9 (Roche, Switzerland). Tau seeds (recombinant and patient brain lysates) were suspended in Opti-MEM (Thermo Fisher, USA), mixed with Multifectam (Promega, USA), incubated at room temperature for 30 min, and introduced into the cells. The medium was replaced with fresh medium after 24-h incubation at 37 °C and 0.2−10 mM lithium (Lithium Chloride, Wako, Japan) was added followed by 48-h incubation.

2.3. Preparation of insoluble tau fraction

Cells were suspended in A68 buffer for the preparation of sarkosyl-soluble and -insoluble tau, as described previously [22]. Briefly, after sonication on ice, the cell homogenate was centrifuged at 100,000×*g* for 20 min. The supernatants were collected as the soluble fraction (Sol). The remaining pellets were resuspended in A68 buffer with 1% Triton X-100 and centrifuged at 100,000×*g* for 20 min. The pellets were resuspended in A68 buffer containing 1% sarkosyl and centrifuged at 100,000×*g* for 20 min. The obtained pellets were used as the sarkosyl-insoluble fraction (Insol). Details of the antibodies are described in Table S2. Band intensities were measured using ImageJ (National Institutes of Health, USA) and standardized against the housekeeping protein GAPDH.

2.4. Preparation of stable EGFP-Tau-CTF24/mCherry-LC3 expressing SH-SY5Y cells and seed induction

SH-SY5Y cells were grown in 6-well plates and transfected with 1 μg/well of the tau expression plasmid (pCDNA3_EGFP-Tau-CTF24) and mCherry-LC3 (pCDNA3_mCherry-LC3). Transfected cells were transferred to a 10-cm dish containing 300 μg/ml of gentamicin-sulfate (G418) (nacalai tesque, Japan) and selection medium was added 24 h post-transfection. After one-month, stable double-labeled cells were plated onto a 96-well plate (single cell/well) using a fluorescence activated cell sorter (BD FACSAria II, USA). Double-labeled stable cells were further confirmed under a fluorescence microscope, grown in selection media, and preserved for further experiments. For immunofluorescence**,** cells were grown on collagen-coated coverslips in 6-well culture dishes. After reaching approximately 80% confluence, the tau seeding, and lithium treatment were carried out as described previously. Cells were fixed with 4% (w/v) paraformaldehyde in PBS, followed by 10 min incubation in 50 mM NH_4Cl/PBS. Cell permeabilization was conducted with 0.2% (v/v) Triton X-100 in PBS (PBST). The cells were washed thrice with 1 × PBST and mounted on micro slides using ProLong Diamond Antifade Mountant with DAPI (Thermo Fisher). Fluorescence images were acquired using a LSM780 confocal microscope (Zeiss, Germany).

2.5. Transmission electron microscopy (TEM)

For TEM analysis, SH-SY5Y cells were grown in 35-mm collagen-coated culture dishes. After 48 h of lithium treatment, cells were fixed with 2.5% glutaraldehyde in 0.1 M phosphate buffer (pH 7.4), followed by post-fixation with 2% OsO_4 in the same buffer. Fixed specimens were dehydrated with a graded series of ethanol and embedded in Epok812 (Oken shoji, Japan). Ultra-thin sections were cut and stained with uranyl acetate and lead citrate. These sections were examined under an HT7700 transmission electron microscope (Hitachi, Japan).

2.6. Malachite green assay (MGA)

Previous reports had described the mechanism of lithium-induced autophagy to be via inhibition of IMPase [20]. IMPase activity was assessed indirectly by measuring inorganic phosphate content by malachite green assay (MGA) [23]. Following the previously described seeding and lithium/L690,330 treatment, A68 buffer-soluble fractions (Sol) of cells were used according to the manufacturer's protocol (Malachite Green Phosphate Detection kit, R&D Systems. Inc. USA). The assay was conducted in 96-well flat-bottom plates and color change was quantified at 620 nm using a spectrophotometer (Molecular Device, USA).

2.7. Data analysis and statistics

Data were analyzed by Student's *t*-test for two-group comparisons after distribution analysis using JMP 12.0 software (SAS Institute, USA). For multi-group comparison, the nonparametric Wilcoxon signed-rank test was used.

3. Results

3.1. Lithium alleviated insoluble tau and altered autophagic markers in presence of AD seeds

To clarify the effect of lithium on clearance of aggregated tau, we applied 10 mM lithium for 48 h after introducing AD brain seeds into Tau-CTF24-overexpressing cells, and the buffer-soluble and sarkosyl-insoluble tau were fractionated thereafter. Western blotting revealed the amount of sarkosyl-insoluble tau to be significantly decreased while the buffer-soluble tau level remained unchanged (Fig. 1A and B). mRNA expression analysis of Tau-CTF24 further confirmed that lithium had no effect on the expression of tau in SH-SY5Y cells (Figs. S1B and C).

We next analyzed a well-established autophagy marker, LC3-II, and found its protein levels to be significantly increased (Fig. 1A, D) after exposure to 10 mM lithium. We also examined an autophagic substrate, namely p62/SQSTM1. The level of p62 was significantly reduced in lithium-treated cells than in untreated AD-seeded cells (Fig. 1A, C). To investigate multiple AD cases, we prepared lysates from two other AD brains (AD 2 and AD 3, Table S1 and Fig. S2). Results obtained were similar to those with AD l lysate (Figs. S2A and D).

To understand the specific interaction of tau with LC3, we conducted confocal laser microscopic studies using our stable SH-SY5Y cells harboring both EGFP-Tau-CTF24 and mCherry-LC3. Upon lithium treatment, the number of cells exhibiting colocalized tau/LC3 puncta increased over that in untreated cells (Fig. 1E and F). These observations were consistent with the results of immunoblot analysis.

TEM analysis revealed that after lithium treatment, the number of autophagic vacuoles (AVs), defined as a double-membraned structure containing undigested cytoplasmic content, remarkably increased in SH-SY5Y cells overexpressing Tau-CTF24 and seeded with AD samples, whereas untreated cells had almost none (Fig. 1G and H). This suggested that lithium treatment reduced tau aggregates through the promotion of autophagy of AD seed-dependent aggregates in SH-SY5Y cells.

We observed similar phenomenon of insoluble tau aggregate clearance, post lithium treatment, using transiently expressed human full-length tau (pCDNA3_4R2N-tau) (Fig. S3A) in SH-SY5Y cells. Immunoblot analysis of insoluble tau and LC3-II with AD and heparin-induced recombinant seeds showed similar effects as that with AD seeds in cells overexpressing Tau-CTF24 (Figs. S3B and C). mRNA expression analysis of full-length tau (4R2N) also confirmed lithium to have no effect on tau expression (Fig. S3D). TEM analysis showed the number of AVs to have increased upon lithium treatment in recombinant tau seed-induced cells (Fig. S3E).

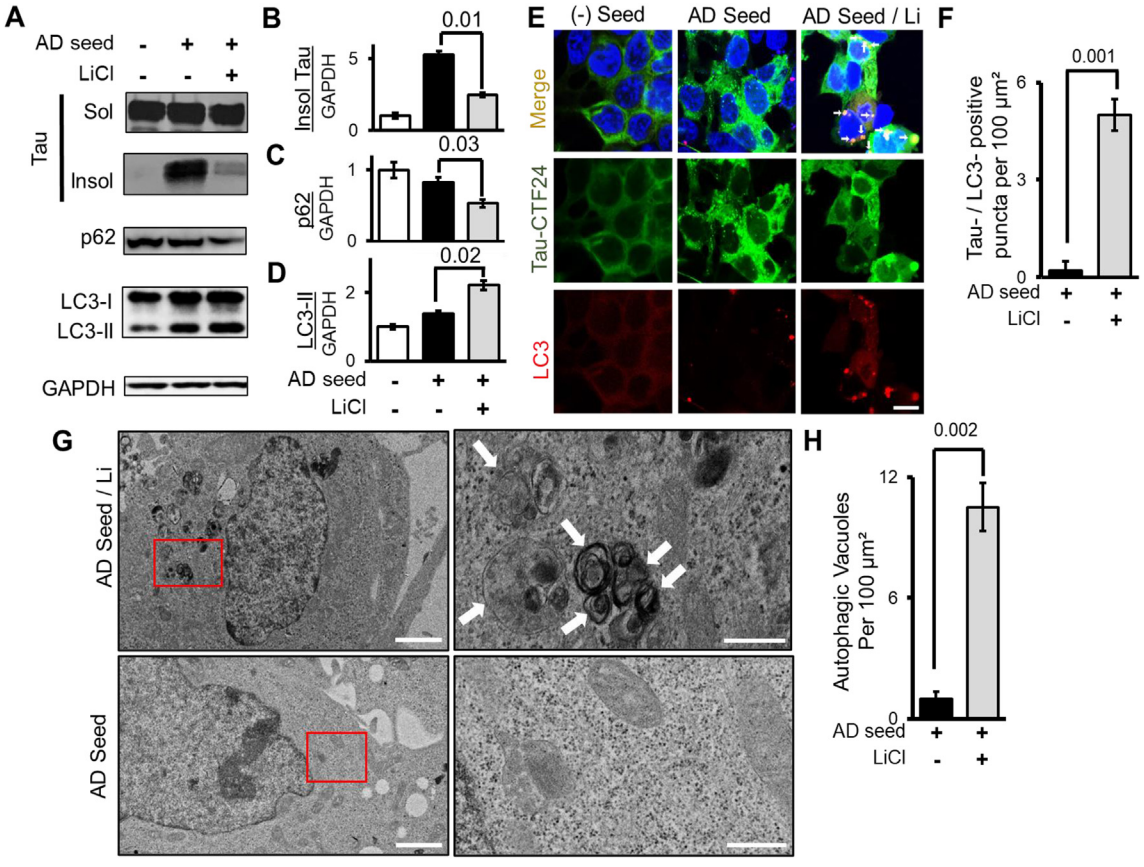

Fig. 1. Lithium treatment reduced insoluble tau and promoted autophagy in AD brain-seeded cells. SH-SY5Y cells overexpressing Tau-CTF24 were treated with AD brain lysates. After a 48-h incubation with 10 mM LiCl, the A68 buffer-soluble (Sol) and sarkosyl-insoluble (Insol) fractions of cells were prepared and analyzed by immunoblotting (A). Quantification of insoluble tau by immunoblotting with T46 antibody that recognizes C-terminal tau (404–441aa) (B). Quantification of the autophagic markers p62 and LC3-II (C, D). Confocal laser microscopic images of EGFP-Tau-CTF24 and mCherry-LC3 (E). Quantification of tau- and LC3- positive puncta in the confocal laser microscopic image per 100 μm^2 (F). TEM analysis revealed that lithium treatment increased autophagic vacuoles (G). Quantification of AVs per 100 μm^2 using >10 different grids by TEM (H). All Western blot quantification was normalized against GAPDH. The two right panels represent high-magnification views of the insets in the left panels. Arrows indicate AVs. Scale bars: 10 µm in E, 500 nm in G at high magnification (right panels), and 2 µm at low magnification (left panels). Data represent the mean ± SEM from four independent experiments (n = 4). Numbers above the bars indicate p-values.

3.2. Strain-specific clearance of insoluble tau and autophagic activity upon lithium treatment

To investigate whether the effects of lithium-induced autophagy differ across seed types, we used brain homogenates of patients with PSP and CBD as seeds. PSP seed-dependent tau aggregates in SH-SH5Y cells reduced insoluble tau and p62, and elevated LC3-II level, as with AD seed (Fig. 2A–D). According to TEM analysis results, PSP-seeded cells treated with lithium had an increased number of AVs (Fig. 2E and F). However, cells with CBD seeds did not show any effect on the amount of insoluble tau or the level of LC3-II after the addition of lithium (Fig. 2G–J), nor did AVs increase in number, as per TEM analysis (Fig. 2K and L).

Additionally, we investigated 2 more PSP and CBD cases each, and confirmed the strain-specific clearance of insoluble tau and autophagic promotion by lithium (Figs. S2B, C, and D). Since we had previously shown the amount of insoluble tau from 3 CBD brains to not be less than that from 3 PSP brains, we concluded that the amount of insoluble tau present in seeds did not influence the lithium-induced autophagy promotion [22].

3.3. Lithium promoted autophagy via myo-inositol monophosphatase (IMPase) inhibition

To explore whether the effects of lithium on autophagy promotion were mediated by the inhibition of IMPase in a strain-specific manner, all three (AD, PSP, and CBD) types of seed-dependent cells were treated with an IMPase inhibitor L690,330 [24]. Forty-eight-hour treatment with L690,330 reduced the amount of insoluble tau, same as in lithium treatment, in AD- and PSP-seeded cells (Fig. 3A, B, and E, F). However, CBD-seeded cells did not show a significant decrease in insoluble tau upon treatment with L690,330 (Fig. 3I, J, and Fig. S4 [A–D]). To evaluate the activity of IMPase, malachite green assay (MGA) was employed; IMPase activity was found to be significantly reduced by lithium and L690,330 treatment in both AD- and PSP-seeded SH-SY5Y cells, whereas it remained unchanged in CBD-seeded cells (Fig. 3C, G, and K). Based on TEM, the number of AVs remarkably increased after L690,330 treatment in AD- and PSP-seeded SH-SY5Y cells while there was no change in the CBD-seeded cells (Fig. 3D, H, and L). The TEM data were consistent with the immunoblot analysis results.

4. Discussion

This study demonstrated that lithium treatment reduced AD seed-dependent tau aggregation in SH-SY5Y cells by promoting autophagy. Lithium-induced autophagy promotion was lower in case of CBD seeds than in case of AD or PSP seeds. The underlying mechanism of lithium-induced autophagy is probably related to low IMPase activity in a seed strain-specific manner (Fig. 4).

In this study, we used human tauopathy brain extracts as seeds to represent seed-dependent aggregation of AD, PSP, and CBD neurodegenerative prions in a cell culture model [8]. We noted an increase in the number of AVs after lithium treatment, using TEM analysis (Fig. 1G and H). Since the presence of AVs is the most important morphological feature of cells with autophagic activity, visualization of these structures by TEM remains the gold standard. Although confocal microscopy and other biochemical techniques have become the leading approaches to investigate autophagy in different settings, they often fail to provide consistent conclusions,

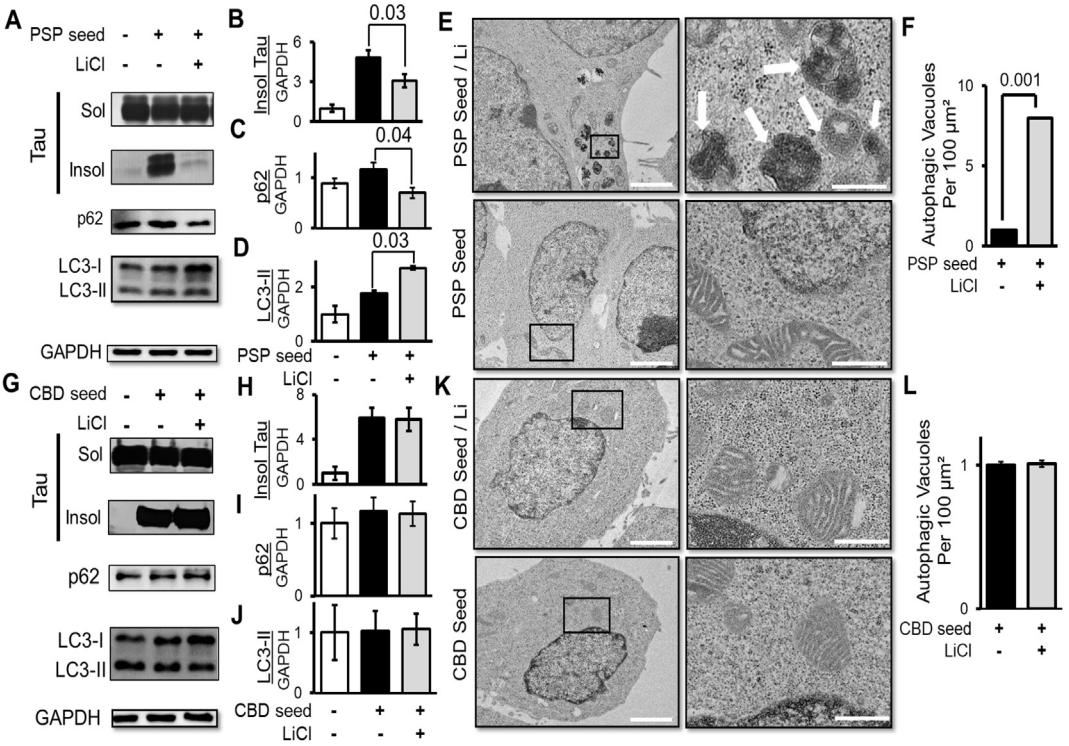

Fig. 2. Strain-specific reduction of aggregated tau by lithium.SH-SY5Y cells overexpressing Tau-CTF24 were treated with PSP or CBD brain lysates. After 10 mM lithium treatment for 48 h, biochemical analysis was performed using T46, LC3-II, and p62 antibodies (A and G). With PSP seeds, lithium treatment reduced the amount of insoluble tau (B) and p62 (C), and increased LC3-II level (D), whereas no difference was noted with CBD seeds (H, I, and J). TEM images of PSP- and CBD-seeded cells, treated or not treated with lithium (E and K). Quantification of AVs in PSP (F) and CBD (L) seeds. The two right panels represent high-magnification views of the insets in the left panels; arrows indicate AVs. All Western blot quantification was normalized against GAPDH. Scale bars: 500 nm in G at high magnification (right panels) and 2 μm at low magnification (left panels). Data represent the mean ± SEM from four independent experiments (n = 4). Numbers above the bars indicate p-values.

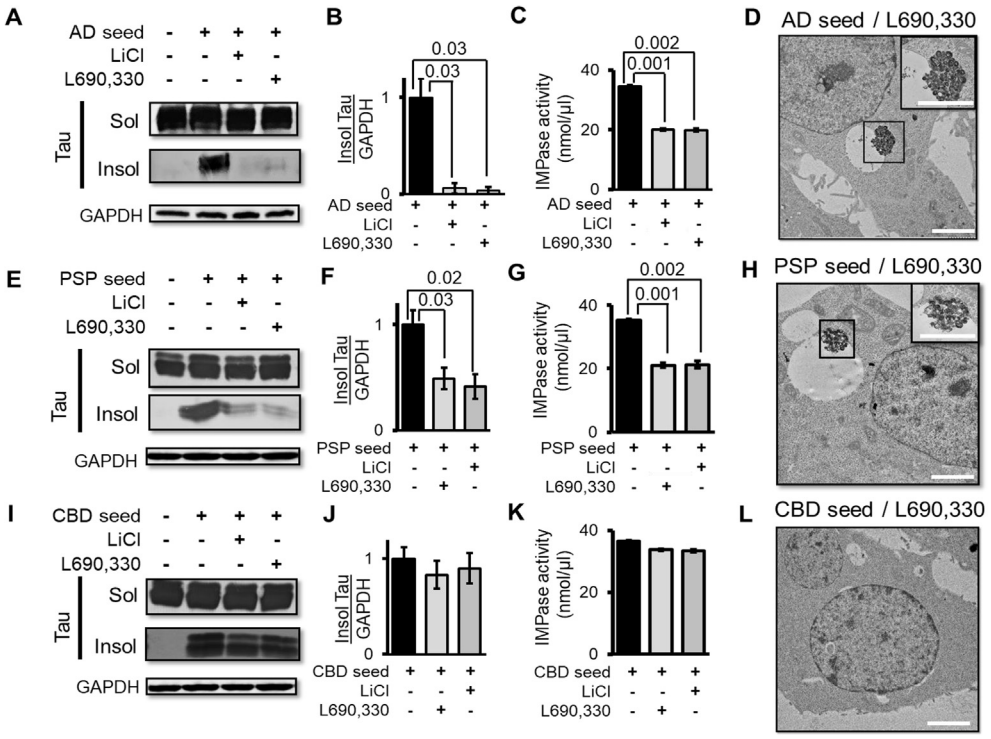

Fig. 3. Lithium-induced autophagy promotion was related to the inhibition of IMPase in a strain-specific manner. SH-SY5Y cells overexpressing Tau-CTF24 were treated with AD, PSP, or CBD brain lysates. After a 48-h incubation with 10 mM LiCl or 100 μM IMPase inhibitor L690,330, the A68 buffer-soluble (Sol) and sarkosyl-insoluble (Insol) fractions of the cells were prepared and analyzed by immunoblotting (A). In AD-seeded cells, L690,330 reduced the amount of insoluble tau (A and B), reduced IMPase activity (C), and increased AVs (D). However, in CBD-seeded cells, L690,330 did not reduce the amount of insoluble tau (E and F), or affect IMPase activity (G), or influence AVs (H). PSP-seeded cells exhibited similar results as AD-seeded cells (I, J, K, and L). Quantification of insoluble tau by immunoblotting with T46 antibody (B, F, and J). TEM imaging of the AVs in cells treated with L690,300 (D, H, and L). The right upper panels represent high-magnification views of the insets. All Western blot quantification was normalized against GAPDH. Scale bars: 500 nm in D, H, and L at high magnification and 2 μm at low magnification. Data represent the mean ± SEM from four independent experiments (n = 4). Numbers above the bars indicate p-values.

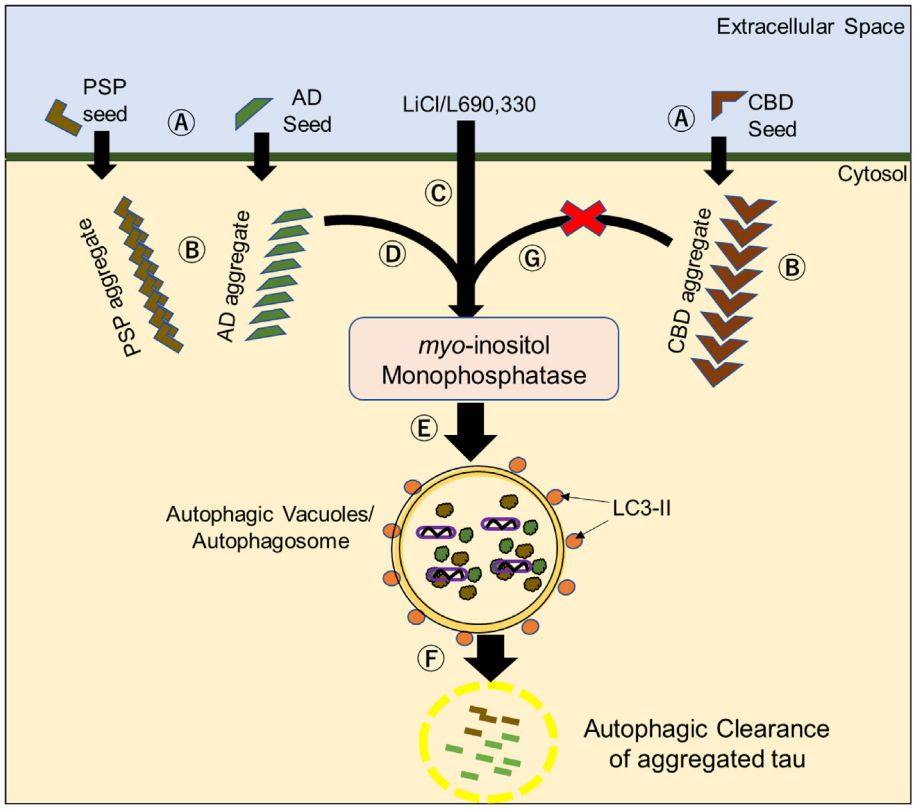

Fig. 4. Schematic illustration of strain-specific clearance of tau aggregates by lithium via autophagy promotion. Tauopathy (AD, CBD, and PSP) seeds enter cells (A) and form tau aggregates (B). Lithium and L690,330 enter the cells and inhibit myo-inositol monophosphatase (C). In AD and PSP aggregates, after inhibition of IMPase by lithium, autophagic membrane formation is enhanced, tau aggregates are sequestered into autophagosome/autophagic vacuoles (D, E), and eventually cleared by autophagic/lysosomal degradation (F). In contrast, CBD aggregates disrupt the inhibitory effect of lithium on IMPase (G), as a result of which, CBD-seed-mediated tau aggregates are not reduced by lithium-induced autophagy.

unless combined with TEM [25]. Furthermore, we confirmed an increase in the number of autophagic puncta and colocalization of Tau/LC3 in the stable SH-SY5Y cells expressing GFP-Tau-CTF24/mCherry-LC3 (Fig. 1D and E). Collectively, our seed-dependent cell models strongly supported the hypothesis that lithium induces degradation of aggregated tau by promoting autophagic flux.

Autophagic clearance of aggregated protein is a dynamic process that involves multiple signaling pathways [17]. IMPase is involved in the synthesis and recycling of inositol via catalysis of the rate-limiting conversion of phosphatidylinositol-3-phosphate (PI3P) into inositol [26]. Reducing intracellular inositol or IP3 levels may induce autophagy [27]. In the present study, treatment with L690,330 increased the clearance of insoluble tau as well as the number of AVs when AD or PSP seeds were introduced (Fig. 3). Furthermore, lithium reduced IMPase activity in the seed-dependent tau aggregation cell models in a strain-specific manner (Fig. 3), confirming the inositol depletion hypothesis [28]. These findings suggested that lithium-induced autophagic clearance of insoluble tau was mediated by IMPase inhibition (Fig. 4).

It was noteworthy that lithium-induced autophagy promotion was less effective with CBD seeds than with AD or PSP seeds (Fig. 2). Recently, cryo-electron microscopy has clarified the difference in tau filament structure between AD and CBD [12–14]. AD filament cores are made of two identical C-shaped protofilaments comprising of residues 306–378 of tau protein, whereas the core of a CBD filament comprises of residues 275–380, adopting a four-layer fold. Since IMPase inhibitor L690,330 was not able to influence IMPase activity in CBD seed-treated cells, unlike in those treated with AD or PSP seeds (Fig. 3), we considered the difference of filament structure to possibly influence enzyme-protein interaction leading to strain-specific lithium-induced autophagy promotion.

One potential limitation of this study is that 10 mM lithium concentration was used in almost all our experiments, as per a previously published paper [29]. Since severe lithium toxicity can occur at a blood level of $\geq$2.0 mM, we used the low concentration condition only (Figs. S5A and B). Although the effects of lithium on tau aggregation decreased in a concentration-dependent manner, even 0.2 mM lithium showed a small reduction in the amount of tau aggregation. This suggested that lithium treatment could be clinically feasible for the treatment of patients with AD, considering that the duration of illness spans over several years, and small effects can accumulate gradually. Another potential limitation is that we performed experiments only on cell cultures, not on live animals. Further studies, examining the lithium effect in mice with brain-injected tauopathy, will be necessary.

In conclusion, the study demonstrated that lithium treatment alleviated tau aggregation in a strain-specific manner in seed-dependent cell models. This possibly implies that lithium may be therapeutically effective in the treatment of specific tauopathies.

Author contributions

MNU performed all biochemical experiments. MNU and ME performed immunohistochemistry and ultrastructural analysis. MNU, ME and SS were involved in study design and data analysis. SK performed TEM sample preparation and discussion. SS, and KI participated in the data discussion. MNU, ME and YM wrote the manuscript. YM and NH supervised the whole study.

Declaration of competing interest

The authors declare that they have no known competing interest in this paper.

Acknowledgements

The authors are grateful to Masashi Takanashi for providing AD, CBD, and PSP brain sections.

Appendix A. Supplementary data

Supplementary data to this article can be found online at https://doi.org/10.1016/j.bbrc.2020.12.113.

Funding

This work was supported by the Japanese Goverment, Ministry of Education, Culture, Sports, Science and Technology (MEXT) KAKENHI [grant number 18K07456].

References

[1] V.M. Lee, M. Goedert, J.Q. Trojanowski, Neurodegenerative tauopathies, Annu. Rev. Neurosci. 24 (2001) 1121–1159, https://doi.org/10.1146/annurev.neuro.24.1.1121.
[2] Y. Motoi, N. Sahara, T. Kambe, N. Hattori, Tau and neurodegenerative disorders, Biomol. Concepts 1 (2010) 131–145, https://doi.org/10.1515/bmc.2010.017.
[3] T. Arai, K. Ikeda, H. Akiyama, T. Nonaka, M. Hasegawa, K. Ishiguro, S. Iritani, K. Tsuchiya, E. Iseki, S. Yagishita, T. Oda, A. Mochizuki, Identification of amino-terminally cleaved tau fragments that distinguish progressive supranuclear palsy from corticobasal degeneration, Ann. Neurol. 55 (2004) 72–79, https://doi.org/10.1002/ana.10793.
[4] K. Arima, Ultrastructural characteristics of tau filaments in tauopathies: immuno-electron microscopic demonstration of tau filaments in tauopathies, Neuropathology 26 (2006) 475–483, https://doi.org/10.1111/j.1440-1789.2006.00669.x.
[5] B. Frost, R.L. Jacks, M.I. Diamond, Propagation of tau misfolding from the outside to the inside of a cell, J. Biol. Chem. 284 (2009) 12845–12852, https://doi.org/10.1074/jbc.M808759200.
[6] S.E. Matsumoto, Y. Motoi, K. Ishiguro, T. Tabira, F. Kametani, M. Hasegawa, N. Hattori, The twenty-four KDa C-terminal tau fragment increases with aging in tauopathy mice: implications of prion-like properties, Hum. Mol. Genet. 24 (2015) 6403–6416, https://doi.org/10.1093/hmg/ddv351.
[7] F. Clavaguera, H. Akatsu, G. Fraser, R.A. Crowther, S. Frank, J. Hench, A. Probst, D.T. Winkler, J. Reichwald, M. Staufenbiel, B. Ghetti, M. Goedert, M. Tolnay, Brain homogenates from human tauopathies induce tau inclusions in mouse brain, Proc. Natl. Acad. Sci. U.S.A. 110 (2013) 9535–9540, https://doi.org/10.1073/pnas.1301175110.
[8] J.L. Guo, S. Narasimhan, L. Changolkar, Z. He, A. Stieber, B. Zhang, R.J. Gathagan, M. Iba, J.D. McBride, J.Q. Trojanowski, V.M. Lee, Unique pathological tau conformers from Alzheimer's brains transmit tau pathology in nontransgenic mice, J. Exp. Med. 213 (2016) 2635–2654, https://doi.org/10.1084/jem.20160833.
[9] S. Narasimhan, J.L. Guo, L. Changolkar, A. Stieber, J.D. McBride, L.V. Silva, Z. He, B. Zhang, R.J. Gathagan, J.Q. Trojanowski, V.M.Y. Lee, Pathological tau strains from human brains recapitulate the diversity of tauopathies in nontransgenic mouse brain, J. Neurosci. : Off. J.Soc. Neurosci. 37 (2017) 11406–11423, https://doi.org/10.1523/JNEUROSCI.1230-17.2017.
[10] G.S. Gibbons, V.M.Y. Lee, J.Q. Trojanowski, Mechanisms of cell-to-cell transmission of pathological tau: a review, JAMA neurology 76 (2019) 101–108, https://doi.org/10.1001/jamaneurol.2018.2505.
[11] M. Goedert, M.G. Spillantini, Propagation of tau aggregates, Mol. Brain 10 (2017) 18, https://doi.org/10.1186/s13041-017-0298-7.
[12] A.W.P. Fitzpatrick, B. Falcon, S. He, A.G. Murzin, G. Murshudov, H.J. Garringer, R.A. Crowther, B. Ghetti, M. Goedert, S.H.W. Scheres, Cryo-EM structures of tau filaments from Alzheimer's disease, Nature 547 (2017) 185–190, https://doi.org/10.1038/nature23002.
[13] W. Zhang, A. Tarutani, K.L. Newell, A.G. Murzin, T. Matsubara, B. Falcon, R. Vidal, H.J. Garringer, Y. Shi, T. Ikeuchi, S. Murayama, B. Ghetti, M. Hasegawa, M. Goedert, S.H.W. Scheres, Novel tau filament fold in corticobasal degeneration, Nature (2020), https://doi.org/10.1038/s41586-020-2043-0.
[14] T. Arakhamia, C.E. Lee, Y. Carlomagno, D.M. Duong, S.R. Kundinger, K. Wang, D. Williams, M. DeTure, D.W. Dickson, C.N. Cook, N.T. Seyfried, L. Petrucelli, A.W.P. Fitzpatrick, Posttranslational modifications mediate the structural diversity of tauopathy strains, Cell 180 (2020) 633–644, https://doi.org/10.1016/j.cell.2020.01.027, e612.
[15] B. Ravikumar, S. Sarkar, J.E. Davies, M. Futter, M. Garcia-Arencibia, Z.W. Green-Thompson, M. Jimenez-Sanchez, V.I. Korolchuk, M. Lichtenberg, S. Luo, D.C. Massey, F.M. Menzies, K. Moreau, U. Narayanan, M. Renna, F.H. Siddiqi, B.R. Underwood, A.R. Winslow, D.C. Rubinsztein, Regulation of mammalian autophagy in physiology and pathophysiology, Physiol. Rev. 90 (2010) 1383–1435, https://doi.org/10.1152/physrev.00030.2009.

[16] R.A. Nixon, The role of autophagy in neurodegenerative disease, Nat. Med. 19 (2013) 983–997, https://doi.org/10.1038/nm.3232.
[17] A.S. Chesser, S.M. Pritchard, G.V. Johnson, Tau clearance mechanisms and their possible role in the pathogenesis of Alzheimer disease, Front. Neurol. 4 (2013) 122, https://doi.org/10.3389/fneur.2013.00122.
[18] F. Guo, X. Liu, H. Cai, W. Le, Autophagy in neurodegenerative diseases: pathogenesis and therapy, Brain Pathol. 28 (2018) 3–13, https://doi.org/10.1111/bpa.12545.
[19] Y. Motoi, K. Shimada, K. Ishiguro, N. Hattori, Lithium and autophagy, ACS Chem. Neurosci. 5 (2014) 434–442, https://doi.org/10.1021/cn500056q.
[20] S. Sarkar, R.A. Floto, Z. Berger, S. Imarisio, A. Cordenier, M. Pasco, L.J. Cook, D.C. Rubinsztein, Lithium induces autophagy by inhibiting inositol monophosphatase, J. Cell Biol. 170 (2005) 1101–1111, https://doi.org/10.1083/jcb.200504035.
[21] A. Heiseke, Y. Aguib, C. Riemer, M. Baier, H.M. Schatzl, Lithium induces clearance of protease resistant prion protein in prion-infected cells by induction of autophagy, J. Neurochem. 109 (2009) 25–34, https://doi.org/10.1111/j.1471-4159.2009.05906.x.
[22] S. Shimonaka, S.E. Matsumoto, M. Elahi, K. Ishiguro, M. Hasegawa, N. Hattori, Y. Motoi, Asparagine residue 368 is involved in Alzheimer's disease tau strain-specific aggregation, J. Biol. Chem. (2020), https://doi.org/10.1074/jbc.RA120.013271.
[23] J. Feng, Y. Chen, J. Pu, X. Yang, C. Zhang, S. Zhu, Y. Zhao, Y. Yuan, H. Yuan, F. Liao, An improved malachite green assay of phosphate: mechanism and application, Anal. Biochem. 409 (2011) 144–149, https://doi.org/10.1016/j.ab.2010.10.025.
[24] G. Sconzo, D. Cascino, G. Amore, F. Geraci, G. Giudice, Effect of the IMPase inhibitor L690,330 on sea urchin development, Cell Biol. Int. 22 (1998) 91–94, https://doi.org/10.1006/cbir.1998.0229.
[25] E.L. Eskelinen, F. Reggiori, M. Baba, A.L. Kovacs, P.O. Seglen, Seeing is believing: the impact of electron microscopy on autophagy research, Autophagy 7 (2011) 935–956, https://doi.org/10.4161/auto.7.9.15760.
[26] Y. Sade, L. Toker, N.Z. Kara, H. Einat, S. Rapoport, D. Moechars, G.T. Berry, Y. Bersudsky, G. Agam, IP3 accumulation and/or inositol depletion: two downstream lithium's effects that may mediate its behavioral and cellular changes, Transl. Psychiatry 6 (2016) e968, https://doi.org/10.1038/tp.2016.217.
[27] K. Pierzynowska, L. Gaffke, Z. Cyske, M. Puchalski, E. Rintz, M. Bartkowski, M. Osiadly, M. Pierzynowski, J. Mantej, E. Piotrowska, G. Wegrzyn, Autophagy stimulation as a promising approach in treatment of neurodegenerative diseases, Metab. Brain Dis. 33 (2018) 989–1008, https://doi.org/10.1007/s11011-018-0214-6.
[28] M.J. Berridge, C.P. Downes, M.R. Hanley, Neural and developmental actions of lithium: a unifying hypothesis, Cell 59 (1989) 411–419, https://doi.org/10.1016/0092-8674(89)90026-3.
[29] R.S. Williams, L. Cheng, A.W. Mudge, A.J. Harwood, A common mechanism of action for three mood-stabilizing drugs, Nature 417 (2002) 292–295, https://doi.org/10.1038/417292a.